

Electronic States and Superconductivity in Multi-layer High- T_c Cuprates

M. Mori, T. Tohyama, and S. Maekawa

Institute for Materials Research, Tohoku University, Sendai 980-8577, Japan

(September 30, 2001)

We study electronic states of multi-layer cuprates in the normal phases as functions of the number of CuO_2 planes and the doping rate. The resonating valence bond (RVB) wave function and the Gutzwiller approximation are used for a two-dimensional multi-layer t - t' - t'' - J model. We calculate the electron-removal spectral functions at $(\pi, 0)$ in the CuO_2 plane next to the surface to understand the angle-resolved photoemission spectroscopy (ARPES) spectra. We find that the tri-layer spectrum is narrower than the bi-layer spectrum but is wider than the mono-layer spectrum. In the tri- and tetra-layer systems, the outer CuO_2 plane has different superconducting amplitude from the inner CuO_2 plane, while each layer in the bi-layer systems has same amplitude. The recent ARPES and NMR experiments are discussed in the light of the present theory.

PACS number: 74.25.Jb, 74.20.-z, 71.10.Fd

I. INTRODUCTION

In studies of high- T_c superconductivity, the number of CuO_2 planes in a unit cell, n , is one of the key factors. It is indicated that the maximum T_c monotonically increases with n and saturates at either $n=3$ or 4. [1,2] The bi-layer compounds have crystallographically equivalent CuO_2 planes, while the tri- and tetra-layer compounds have inequivalent planes, i.e., the outer-pyramidal-coordinated-planes (OP) and the inner-square-coordinated-planes (IP). By calculating the Madelung energy for Bi- and Tl- compounds in the point charge model, it was shown that the hole density of the IP, $N_h(\text{IP})$, is lower than that of the OP, $N_h(\text{OP})$, since the IP is sandwiched by Ca sheets with positive charge. [3,4] It was also argued that a hole density difference $\Delta N_h \equiv N_h(\text{OP}) - N_h(\text{IP})$ becomes large by increasing n and controls the superconducting phases. [5-7]

Such hole distribution among the CuO_2 layers was observed above T_c by the ^{17}O - and ^{63}Cu -nuclear-magnetic-resonance

(NMR) measurement for Pb doped $\text{Bi}_2\text{Sr}_2\text{Ca}_2\text{Cu}_3\text{O}_{10+y}$ (Bi2223) [8,9] and for $\text{HgSr}_2\text{Ca}_2\text{Cu}_3\text{O}_{10+y}$ (Hg1223). [10,11] These studies showed that the IP has smaller carrier density and larger antiferromagnetic (AF) correlation than the OP. Kotegawa *et al.* systematically estimated the hole density in each layer by the ^{63}Cu Knight shift in $\text{HgBa}_2\text{Ca}_{n-1}\text{Cu}_n\text{O}_{2n+2+y}$ and $\text{CuBa}_2\text{Ca}_{n-1}\text{Cu}_n\text{O}_{2n+4-y}$. [12] By use of an empirical relation between the Knight shift at room temperature and the hole density, which was deduced from the nuclear quadruple resonance (NQR) frequency, [13] they found that the hole density difference among the layers increases as either a total carrier content δ_{total} or n increases.

As regards an inter-layer hopping, the bilayer splitting was shown by band calculations [14-16] and clearly observed by the angle-resolved-photoemission spectroscopy

(ARPES) in $\text{Bi}_2\text{Sr}_2\text{CaCu}_2\text{O}_{8+y}$ (Bi2212) above T_c . [17-19] However, a tri-layer splitting in Bi2223 has not been observed. [20,21] To understand the electronic states in the multi-layer cuprates, it is necessary to clarify the reason why the tri-layer splitting is not clearly observed, although the bi-layer splitting is distinguishable.

In the present paper, the electron-removal spectral function is calculated in a two-dimensional multi-layer t - t' - t'' - J model at zero temperature by using the resonating valence bond (RVB) wave function and the Gutzwiller approximation. We study the n -dependence of the single-particle excitations including the inter-layer hopping which connects the chemically different CuO_2 planes for $n \geq 3$. Since the ARPES measurement is sensitive to a surface of sample due to a short escape depth of outgoing electron, the spectra in the tri- and tetra-layer compounds should be dominated by the OP's contribution. Moreover, the spectra depend on the incident photon energy $h\nu$ and the photoemission matrix element. [22-25] The spectra in the bi-layer systems have two peaks composed of the bonding (B) and anti-bonding (AB) bands, while the spectra in tri-layer systems have three peaks. We find that the splitting between the two dominant peaks in the tri-layer system is smaller than the bi-layer splitting. Then, the tri-layer spectrum is narrower than the bi-layer spectrum but is wider than the mono-layer spectrum.

In the superconducting (SC) phase, Tokunaga *et al.* studied the temperature-dependence of the Knight shift (K_s) and the nuclear spin-lattice relaxation rate ($1/T_1$) of ^{63}Cu in the tetra-layer compound, $(\text{Cu}_{0.6}\text{C}_{0.4})\text{Bi}_2\text{Sr}_2\text{Ca}_3\text{Cu}_4\text{O}_{12+y}$ [26] and found two characteristic temperature associated with the IP and the OP, $T_0(\text{IP})$ and $T_0(\text{OP})$. Both K_s and $1/T_1$ in the IP markedly decrease below $T_0(\text{IP})=117\text{K}$, while those in the OP moderately decrease below $T_0(\text{IP})=117\text{K}$, but markedly decrease below $T_0(\text{OP})=60\text{K}$. These results suggest that a bulk SC transition set in at 117K but the temperature-dependence of SC amplitude in the OP

is different from the BCS theory. Such a non-BCS amplitude is found in a two-band system where the SC amplitude in one band is different from that in the other band, and these bands are coupled each other by a pair-transfer interaction. [27] The two kinds of T_0 's are observed in the tetra-layer compounds, while it is not found in the tri-layer compounds. [12] We calculate the SC amplitude of each layer and find that the outer CuO_2 plane in both the tri- and tetra-layer systems has different SC amplitude from the inner CuO_2 plane. In our calculations, the difference of SC amplitude in the tri-layer systems is comparable to that in the tetra-layer systems. We consider that the $T_0(\text{IP})$ different from $T_0(\text{OP})$ could be observed also in the tri-layer compounds.

The rest of this paper is organized as follows. In Sec. II, we introduce the multi-layer t - t' - t'' - J model that includes the inter-layer hopping and the site-potential. Section III is devoted to show the electronic states in the normal phases and the electron-removal spectral functions. The layer-dependence of superconducting amplitudes is shown in Sec. IV. Summary and discussions are given in Sec. V.

II. THEORETICAL MODEL

We examine the electronic state in the characteristic block of n CuO_2 layers. The Hamiltonian of each layer is given by,

$$\begin{aligned} \hat{H}_{intra} = & -t \sum_{\alpha, \langle ij \rangle_{1st}, \sigma} \hat{c}_{\alpha, j, \sigma}^\dagger \hat{c}_{\alpha, i, \sigma} - t' \sum_{\alpha, \langle ij \rangle_{2nd}, \sigma} \hat{c}_{\alpha, j, \sigma}^\dagger \hat{c}_{\alpha, i, \sigma} \\ & - t'' \sum_{\alpha, \langle ij \rangle_{3rd}, \sigma} \hat{c}_{\alpha, j, \sigma}^\dagger \hat{c}_{\alpha, i, \sigma} + H.c. \\ & + J \sum_{\alpha, \langle ij \rangle_{1st}} \vec{S}_{\alpha, i} \cdot \vec{S}_{\alpha, j}, \end{aligned} \quad (1)$$

where $\hat{c}_{\alpha, i, \sigma} = c_{\alpha, i, \sigma}(1 - n_{\alpha, i, -\sigma})$ is the annihilation operator of an electron in the α layer with spin σ at site i with the constraint of no double occupancy, and $n_{\alpha, i, -\sigma}$ and $\vec{S}_{\alpha, i}$ are the charge and the spin operators, respectively. The summations $\langle ij \rangle_{1st}$, $\langle ij \rangle_{2nd}$ and $\langle ij \rangle_{3rd}$ run over first, second and third nearest-neighbor sites, respectively. The values of the parameters are as follows; $J = 0.14$ eV, $t/J = 2.5$, $t'/J = -0.85$ and $t''/J = 0.575$. [28,29]

The inter-layer hopping has the dispersion relation, [14]

$$\epsilon_\perp(k) = -\frac{t_\perp}{4} (\cos(k_x) - \cos(k_y))^2, \quad (2)$$

which is obtained by integrating out the high-energy degrees of freedom from the Hamiltonian reproducing the full LDA calculation. [15,16] We adopt Eq. (2) for $n \geq 2$

and $t_\perp/J = 1.0$, [14–18] and write the Hamiltonian of the inter-layer hopping as,

$$\hat{H}_{inter} = \sum_{\alpha \neq \beta, k, \sigma} \epsilon_\perp(k) \left(\hat{c}_{\alpha, k, \sigma}^\dagger \hat{c}_{\beta, k, \sigma} + H.c. \right), \quad (3)$$

where α and β are the layer indices.

To describe the hole distribution among the layers, we introduce a site-potential, W , in the IP's as,

$$\hat{H}_{site} = W \sum_{\gamma=\text{in}, k, \sigma} \hat{c}_{\gamma, k, \sigma}^\dagger \hat{c}_{\gamma, k, \sigma} = W \sum_{\gamma=\text{in}} n_\gamma, \quad (4)$$

where γ indicates the IP index. The value of W should be negative. For simplicity, W is taken to be independent of the hole densities.

The total Hamiltonian is,

$$\hat{H} = \hat{H}_{intra} + \hat{H}_{inter} + \hat{H}_{site}. \quad (5)$$

Since this Hamiltonian includes the constraint of no double occupancy, we adopt the Gutzwiller approximation and statistically average the constraint before variational calculation. Details of calculations are summarized in Appendix. In the normal phases, the order parameter,

$$\chi_{\alpha, \tau} \equiv \frac{1}{N} \sum_i \langle c_{\alpha, i, \uparrow}^\dagger c_{\alpha, i+\tau, \uparrow} + c_{\alpha, i, \downarrow}^\dagger c_{\alpha, i+\tau, \downarrow} \rangle, \quad (6)$$

is introduced and referred to as 'uniform RVB' (u-RVB). In addition to this, in the SC phase, the order parameter,

$$B_{\alpha, \tau} = -\frac{1}{N} \sum_i \langle c_{\alpha, i, \uparrow} c_{\alpha, i+\tau, \downarrow} - c_{\alpha, i, \downarrow} c_{\alpha, i+\tau, \uparrow} \rangle, \quad (7)$$

is included and referred to as 'singlet RVB' (s-RVB).

Then, we obtain the following mean-field Hamiltonian, which is numerically solved,

$$\begin{aligned} \hat{H}_{RVB} - \mu N = & \sum_{\alpha, k, \sigma} \xi_\alpha(k) c_{\alpha, k, \sigma}^\dagger c_{\alpha, k, \sigma} \\ & + \sum_{\alpha \neq \beta, k, \sigma} \epsilon_\perp(k) c_{\alpha, k, \sigma}^\dagger c_{\beta, k, \sigma} + \sum_{\gamma, k, \sigma} W c_{\gamma, k, \sigma}^\dagger c_{\gamma, k, \sigma} \\ & - \sum_{k, \tau=x, y} \frac{3}{4} J \left[B_{\alpha, \tau}^* \cos(k_\tau) c_{\alpha, -k, \downarrow} c_{\alpha, k, \uparrow} \right. \\ & \quad \left. + B_{\alpha, \tau} \cos(k_\tau) c_{\alpha, k, \uparrow}^\dagger c_{\alpha, -k, \downarrow}^\dagger \right], \end{aligned} \quad (8)$$

$$\begin{aligned} \xi_\alpha(k) = & - \left[2\hat{t} \{ \cos(k_x) + \cos(k_y) \} + 4\hat{t}' \cos(k_x) \cos(k_y) \right. \\ & \left. + 2\hat{t}'' \{ \cos(2k_x) + \cos(2k_y) \} \right] - \mu \\ & - \frac{3}{4} \hat{J} \{ \chi_{\alpha, x} \cos(k_x) + \chi_{\alpha, y} \cos(k_y) \}, \end{aligned} \quad (9)$$

$$\chi_{\alpha, \tau} = \frac{1}{N} \sum_k \sum_\sigma \cos(k_\tau) \langle c_{\alpha, k, \sigma}^\dagger c_{\alpha, k, \sigma} \rangle, \quad (10)$$

$$B_{\alpha, \tau} = -\frac{1}{N} \sum_k 2 \cos(k_\tau) \langle c_{\alpha, k, \uparrow} c_{\alpha, -k, \downarrow} \rangle, \quad (11)$$

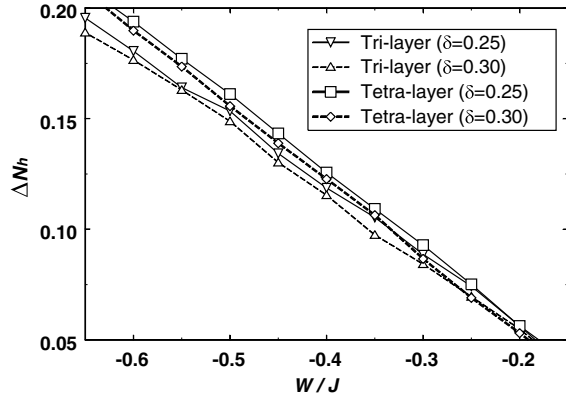


FIG. 1. W -dependence of ΔN_h in the u-RVB state for the tri-layer and the tetra-layer with $\delta = 0.25$ and 0.3 . The values of the parameters are, $J = 0.14$ eV, $t/J = 2.5$, $t'/J = -0.85$, $t''/J = 0.575$ and $t_\perp/J = 1.0$. The averaged doping rate δ is defined as, $\delta = \delta_{total}/n$, in which δ_{total} is a total hole density in a unit cell.

where μ is the chemical potential and N is the total electron number. The even parity is imposed on $\chi_{\alpha,\tau}$. The k -summations are carried out on 160×160 points in the first Brillouin zone.

III. ELECTRONIC STATES IN NORMAL PHASES

We study single-particle excitations to clarify the electronic states in the normal phases. The characteristics of multi-layer systems are manifest at $(\pi, 0)$ in the dispersion relations, since the inter-layer splitting is largest at this point according to Eq. (2). The electron-removal spectral functions at $(\pi, 0)$ are shown in this section. The averaged doping rate δ is defined as $\delta = \delta_{total}/n$, in which δ_{total} is a total hole density in the characteristic block of n CuO₂ layers. We choose $\delta = 0.25$ or 0.3 , below. These values of δ are useful to study the n -dependence of the single-particle excitations, since the ARPES spectra at $(\pi, 0)$ show sharp quasiparticle peaks for a large doping rate. On the other hand, the ARPES spectra become broad and dull by decreasing the doping rate. [30,31]

Before proceeding to the study of ARPES spectrum, it is necessary to determine the value of W that is still a free parameter. We calculate ΔN_h as a function of W in the u-RVB state of tri- and tetra-layer systems with $\delta = 0.25$ and 0.3 . The results are shown in Fig. 1. We determine a value of W by comparing Fig. 1 to the results obtained by Kotegawa *et al.* [12] in NMR measurement. Their results of ΔN_h in the tri- and tetra-layer samples are fitted by the following equations:

$$\text{Tri-layer; } \Delta N_h = -0.130 + 0.759 \delta, \quad (12)$$

$$\text{Tetra-layer; } \Delta N_h = -0.150 + 0.934 \delta. \quad (13)$$

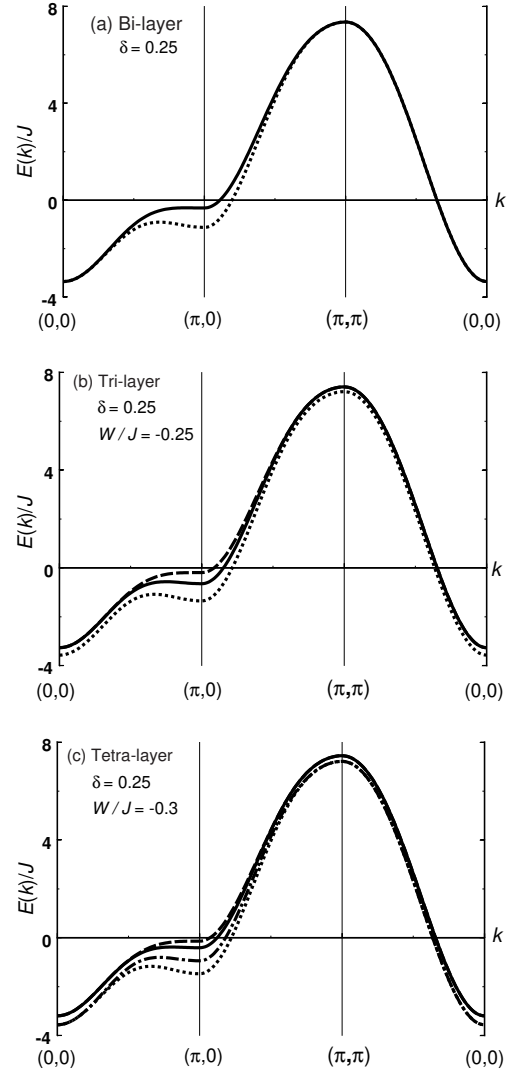


FIG. 2. Dispersion relations of (a) bi-layer, (b) tri-layer, and (c) tetra-layer systems for $\delta = 0.25$ in the u-RVB state. The values of the parameters are, $J = 0.14$ eV, $t/J = 2.5$, $t'/J = -0.85$, $t''/J = 0.575$ and $t_\perp/J = 1.0$.

By using Eqs. (12) and (13), the values of W that reproduce the NMR results are determined as,

Tri-layer;

$$\begin{cases} \delta = 0.25 \rightarrow \Delta N_h = 0.06 \rightarrow W/J = -0.25, \\ \delta = 0.30 \rightarrow \Delta N_h = 0.10 \rightarrow W/J = -0.35, \end{cases} \quad (14)$$

Tetra-layer;

$$\begin{cases} \delta = 0.25 \rightarrow \Delta N_h = 0.08 \rightarrow W/J = -0.30, \\ \delta = 0.30 \rightarrow \Delta N_h = 0.13 \rightarrow W/J = -0.45. \end{cases} \quad (15)$$

The dispersion relations of tri- and tetra-layer systems are plotted together with the bi-layer system ($W = 0$) in Fig. 2 for $\delta = 0.25$. Since the inter-layer hopping is given by Eq. (2), the dispersion relations in the bi-layer system are degenerate in the $(0,0)$ - (π,π) direction and the splitting becomes maximum at $(\pi, 0)$. The band

with lower-binding energy indicated by the solid line in Fig. 2(a) is the AB band and the other one is the B band. The bi-layer splitting at $(\pi,0)$ for $\delta = 0.25$ is $0.8J$, which is given by $2t_{\perp}g_t$. Most of experiments [17–19,22,23] and band calculations [15,16] show two hole-like Fermi surfaces consistent with our dispersion relation. On the other hand, there are experimental [32] and theoretical studies [33] suggesting an electron-like Fermi surface, where the AB band crosses the Fermi level between $(0,0)$ and $(\pi,0)$. Such a dispersion relation would be achieved by small changes of parameters. In the tri-layer system, there exist three bands. Among them, one of the bands indicated by the dotted line in Fig. 2(b) is separated from the other two in the whole Brillouin zone due to the site potential. The middle band shown by the solid line in Fig. 2(b) is composed of only the OP's degrees of freedom as, $(|OP_1\rangle - |OP_2\rangle)/\sqrt{2}$, where $|OP_1\rangle$ and $|OP_2\rangle$ indicate the wave functions in the outer planes. We refer to this band as 'antisymmetric (AOP) band'. The wave functions of remaining two bands are $f(W)(|OP_1\rangle + |OP_2\rangle)/\sqrt{2} \pm g(W)|IP\rangle$, where $|IP\rangle$ indicates the IP's wave function. The coefficients $f(W)$ and $g(W)$ are functions of W . The positive (negative) sign corresponding to the dotted (broken) line in Fig. 2(b) is referred to as 'IP band' ('symmetric (SOP) band'). In the tetra-layer system, OP's and IP's combine to give symmetric and antisymmetric combinations as, $|OP_{\pm}\rangle = (|OP_1\rangle \pm |OP_2\rangle)/\sqrt{2}$ and $|IP_{\pm}\rangle = (|IP_1\rangle \pm |IP_2\rangle)/\sqrt{2}$. The four bands shown in Fig. 2(c) have the following combinations at $(\pi,0)$ from the top to the bottom, $|\alpha\rangle = f_1|IP_{-}\rangle + g_1|OP_{-}\rangle$, $|\beta\rangle = f_2|IP_{+}\rangle - g_2|OP_{+}\rangle$, $|\gamma\rangle = f_3|IP_{-}\rangle - g_3|OP_{-}\rangle$ and $|\delta\rangle = f_4|IP_{+}\rangle + g_4|OP_{+}\rangle$, where f_i and g_i ($i = 1 \sim 4$) are functions of W .

In the following, we assume that the ARPES experiments in Bi-compounds mainly detect the single-particle excitation in the CuO_2 plane next to the BiO layer. The ARPES measurement is sensitive to a surface of sample due to a short escape depth of outgoing electron, which is about 10 \AA or less depending on its kinetic energy in the range of $20 \sim 200 \text{ eV}$. [34] The cleaved surface is considered to be the Bi-O layer, from which the distance to the IP of tri-layer compounds is also about 10 \AA . [1,2] Therefore, the ARPES spectra in the tri- and tetra-layer compounds should be dominated by the OP's contribution. Moreover, the spectra depend on the incident photon energy $h\nu$ and the photoemission matrix element. [22–25] In the case of overdoped bi-layer samples, an anti-bonding (AB) band has a sharp peak at $(\pi,0)$ for $h\nu \sim 22 \text{ eV}$. Although a bonding (B) band is unclear for $h\nu \sim 22 \text{ eV}$, it becomes clear for $h\nu \sim 32 \text{ eV}$ [23] and 47 eV . [22]

The n -dependence of the OP contributions in the electron-removal spectral function, $A^-(k, \omega)$, at $(\pi,0)$ is plotted in Fig. 3 for $t_{\perp}/J = 1.0$. The energy is measured from the Fermi level. In the bi-layer system, the two quasiparticle peaks clearly separate each other for both

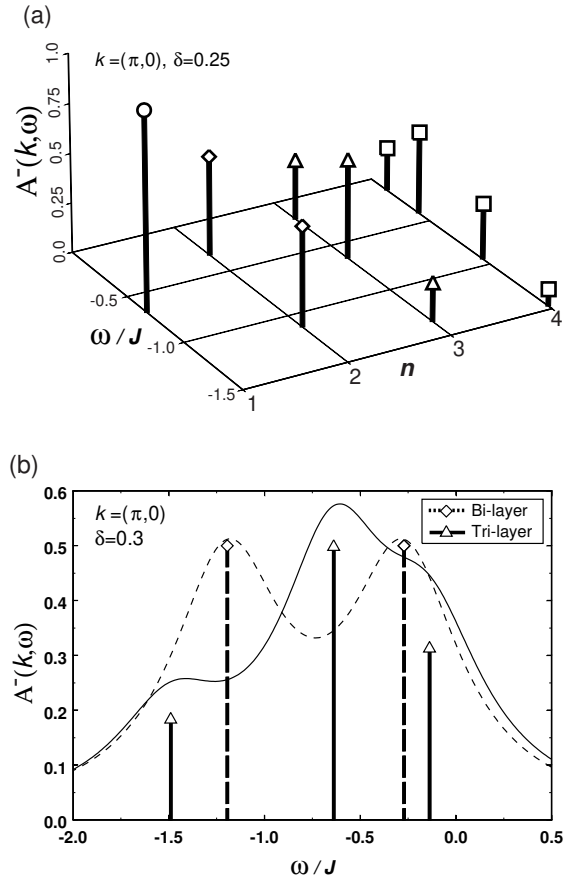


FIG. 3. The n -dependence of the electron-removal spectral function in the normal phase for $J = 0.14 \text{ eV}$, $t/J = 2.5$, $t'/J = -0.85$, $t''/J = 0.575$ and $t_{\perp}/J = 1.0$. The components in the CuO_2 plane nearest to the surface are plotted (a) on the n - ω plane for $\delta = 0.25$, and (b) as functions of ω for $\delta = 0.30$ for the bi- and tri-layer systems. The thin solid (broken) curve is obtained by performing a Lorentzian broadening with a width of $0.35J$ for the δ -functions in the bi- (tri-) layer system. In (a) and (b), the values of W follow Eqs. (14) and (15).

doping rates. The peak with lower-binding energy is the AB band and the other is the B band. In the tri-layer system, the OP's combine to give symmetric and antisymmetric combinations, the latter of which is the AOP-band as defined above and is located at $\omega/J = 0.64$. Only the former can hybridize with the IP, and produces the SOP-band ($\omega/J = 0.14$) and the IP-band ($\omega/J = 1.49$). The total splitting in the tri-layer compound ($\Delta\omega/J = 1.35$) is larger than in the bilayer compound ($\Delta\omega/J = 0.9$), but the SOP-AOP splitting ($\Delta\omega/J = 0.5$) is smaller than the bilayer-splitting. Therefore, the tri-layer spectrum seems to be narrower than the bi-layer spectrum as shown in Fig. 3(b), in which the appropriate broadening is given.

As listed in Table I, the ratios of peak intensities in the OP is, SOP:AOP:IP $\sim 3:5:2$. If the electron escape depth is longer than 10 \AA and the IP can contribute to the ARPES spectral weight, the ratios become

SOP:AOP:IP \sim 7:5:8 from Table I. Therefore, it might be possible to estimate the electron escape depth by comparing a distribution of spectral weight observed in experiment with theoretical one.

TABLE I. The binding energies and the ARPES spectral weights at $k = (\pi, 0)$ in a tri-layer compound for $\delta=0.3$. Each contribution from the IP and the OP is listed.

	ω/J	OP*	IP**
SOP-band	0.14	0.31	0.37
AOP-band	0.64	0.50	0.00
IP-band	1.49	0.19	0.63

* a CuO₂ layer nearest to the surface ** a CuO₂ layer next nearest to the surface

Each spectral weight in the tetra-layer compound is listed in Table. II. The dominant three peaks in the OP,

TABLE II. The binding energies and the ARPES spectral weights at $k = (\pi, 0)$ in a tetra-layer compound for $\delta=0.3$. Each contribution from the IP and the OP is listed.

	ω/J	OP*	IP**
α -band	0.08	0.25	0.25
β -band	0.35	0.43	0.07
γ -band	1.00	0.25	0.25
δ -band	1.65	0.07	0.43

* a CuO₂ layer nearest to the surface ** a CuO₂ layer next nearest to the surface

i.e., α -, β - and γ -band, may result in a broad peak due to the line overlap. Including the IP contribution, it may become more difficult to distinguish the peaks.

IV. SUPERCONDUCTING AMPLITUDES

In this section, we consider the superconducting (SC) state, where the s-RVB state is included in addition to the u-RVB state. As observed in the tetra-layer compounds by NMR experiment, the IP and the OP have different T_0 's, which are ascribed to the different hole concentration in each layer. [26] In the tri-layer compounds, the different T_0 's are not still found, [12] although there is a finite ΔN_h , which is smaller than ΔN_h in the tetra-layer compounds. To understand the SC state in the multi-layer cuprates, we calculate the SC amplitude in each layer defined as $|g_t B_{\alpha,\tau}|$, and show the n -dependence. In the following, we assume that all CuO₂ layers are in the SC phase, and the value of W in the SC phase is the same as that in the normal phase. The results are shown in Fig. 4. The SC gap has the $d_{x^2-y^2}$ -symmetry in each layer for any n . The OP's in both the tri- and tetra-layer systems have different superconducting amplitude from the IP, while each layer in the bi-layer systems has the same amplitude. For $n \geq 3$, the difference of SC amplitude slightly increases with increasing n . Since the

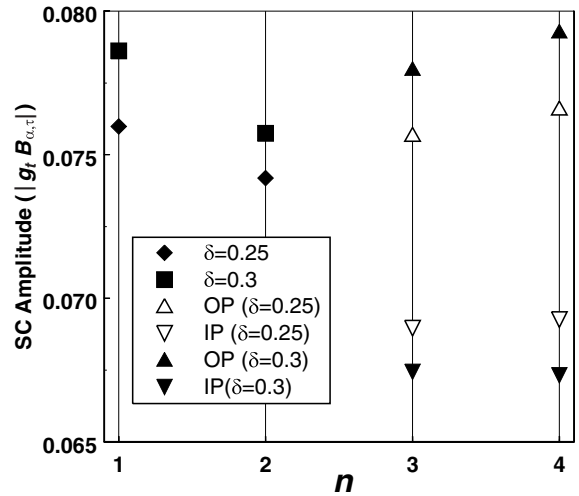


FIG. 4. The n dependence of the SC amplitude at $\delta = 0.3$. For $n \geq 3$, the up- and down-triangle indicate the amplitude in the OP and the IP, respectively. At $n=2$, both layers have the same amplitude. The value of parameters are, $J = 0.14$ eV, $t/J = 2.5$, $t'/J = -0.85$, $t''/J = 0.575$ and $t_{\perp}/J = 1.0$. The values of W follow Eqs. (14) and (15).

difference in the tri-layer systems is comparable to that in the tetra-layer systems, the different T_0 could be observed in experiment.

We note that, although the SC amplitude is larger in the OP than the IP as seen in Fig. 4, the relative magnitude depends on the intra-layer's parameters, which modify the phase diagram of ground state in the mono-layer system. [35] In the present calculation, moreover, the site-potential is fixed at the value in the normal phase. It is also possible that the site-potential depends on the hole densities and is determined self-consistently. If such mechanisms are taken into account, the hole distribution among the layers may change below T_c and the valence of SC amplitudes can be modified. These possibilities are studied elsewhere.

We did not mention quasiparticle excitations in the SC phase. The coherent SC peak in Bi2212 seems to split into two peaks. [17] There are some interpretations of the bi-layer splitting in the SC phase. [17,33] To clarify its origin, more experimental studies on the multi-layer cuprates are needed.

V. SUMMARY

We have studied the electronic states and the superconductivity in multi-layer cuprates by use of the resonating valence bond wave function and the Gutzwiller approximation for the two-dimensional multi-layer t - t' - t'' - J model. In this model, the one-particle hopping connects the chemically different CuO₂ planes in the tri- and tetra-layer systems. We calculated the electron-removal

spectra in the CuO₂ plane next to the BiO layer, since the ARPES is sensitive to the surface of sample. We find that the ARPES spectra in the tri-layer systems at $(\pi, 0)$ should be wider than that in the bi-layer systems, and narrower than that in the mono-layer systems. This is consistent with recent experimental data. [36]

The superconducting (SC) amplitude of each layer is shown as a function of n . In bi-layer system, both layers have the same SC amplitude. In tri- and tetra-layer systems, the SC amplitude of the OP is different from that in the IP due to the different hole concentration. Such a difference could be observed as two different T_0 also in the tri-layer compounds.

ACKNOWLEDGMENTS

The authors would like to thank Z. -X. Shen and D. L. Feng for valuable discussions. This work was supported by the Grant-in-Aid from Ministry of Education, Culture, Sports, Science and Technology of Japan, and CREST. One of authors (S. M.) acknowledges support of the Humboldt Foundation.

GUTZWILLER APPROXIMATION AND RVB WAVE FUNCTION IN MULTI-LAYER SYSTEMS

The RVB-mean-field theory with the Gutzwiller approximation showed that the $d_{x^2-y^2}$ wave superconductivity can be stabilized in the two-dimensional t - J model. [37] The Gutzwiller approximation has been recently generalized to the coexistent state of the d-wave SC and AF order. [38] In this section, we summarize the process to treat the constraint within this approximation.

Explicitly describing the constraint, the Hamiltonian Eq. (5) has the following relation to the non-constrained Hamiltonian,

$$\hat{H} = P_G H P_G. \quad (16)$$

where P_G is the Gutzwiller's projection operator and defined as,

$$P_G = \prod_i (1 - \hat{n}_{i\uparrow} \hat{n}_{i\downarrow}). \quad (17)$$

We assume the projected RVB wave function,

$$|\psi\rangle = P_G |\psi_0(\chi_{\alpha,\tau}, B_{\alpha,\tau}, \mu)\rangle, \quad (18)$$

where $\chi_{\alpha,\tau}$ and $B_{\alpha,\tau}$ are the variational parameters relating to u-RVB and s-RVB, respectively, and $|\psi_0(\chi_{\alpha,\tau}, B_{\alpha,\tau}, \mu)\rangle$ is a mean-field wave function with u-RVB and s-RVB orders. Using these notations, the variational energy $E_{\text{var}} = \langle \hat{H} \rangle$ is rewritten as $E_{\text{var}} = \langle H \rangle_0$, where the parameters t and J in \hat{H} are replaced with

$$\begin{aligned} \hat{t} &= g_t \cdot t, \quad \hat{t}' = g_t \cdot t', \quad \hat{t}'' = g_t \cdot t'', \quad \hat{t}_\perp = g_t \cdot t_\perp, \\ \hat{J} &= g_J \cdot J, \end{aligned} \quad (19)$$

and

$$g_t = 2\delta/(1 + \delta), \quad g_J = 4/(1 + \delta)^2. \quad (20)$$

In the Gutzwiller approximation, the effects of the projection are statistically averaged and renormalized into the expectation values as follows:

$$\langle c_{i\sigma}^\dagger c_{j\sigma} \rangle = g_t \langle c_{i\sigma}^\dagger c_{j\sigma} \rangle_0, \quad \langle \vec{S}_i \cdot \vec{S}_j \rangle = g_s \langle \vec{S}_i \cdot \vec{S}_j \rangle_0, \quad (21)$$

where $\langle \cdots \rangle_0$ represents the expectation value in terms of $|\psi_0\rangle = |\psi_0(\chi_{\alpha,\tau}, B_{\alpha,\tau}, \mu)\rangle$, and $\langle \cdots \rangle$ represents the normalized expectation value in $|\psi\rangle = P_G |\psi_0\rangle$;

$$\langle \hat{O} \rangle \equiv \frac{\langle \psi | \hat{O} | \psi \rangle}{\langle \psi | \psi \rangle} = \frac{\langle \psi_0 | P_G \hat{O} P_G | \psi_0 \rangle}{\langle \psi_0 | P_G P_G | \psi_0 \rangle}. \quad (22)$$

By considering the renormalization factors of coupling constant, the remaining work is to solve the self-consistent equations, in which the renormalization factors are also determined self-consistently. In the multi-layer systems, the constraint is included in the inter-layer hopping and renormalizes t_\perp . Eder *et al.* numerically showed that the t_\perp is renormalized by an in-plane quasi-particle weight. [39] Such an effect is reproduced by the Gutzwiller factor, g_t .

Here, we summarize the eigenvalue problem in the SC state of multi-layer systems. [40] Neglecting the details, the Hamiltonian generally has the following form,

$$\begin{aligned} H &= \sum_{\alpha,\beta,k,\sigma} A c_{\alpha,k,\sigma}^\dagger c_{\beta,k,\sigma} \\ &+ \sum_{\alpha,k} \left(B^* c_{\alpha,-k,\downarrow} c_{\alpha,k,\uparrow} + B c_{\alpha,k,\uparrow}^\dagger c_{\alpha,-k,\downarrow}^\dagger \right), \\ &= \sum_k \phi^\dagger \begin{pmatrix} A & B \\ B^* & -A^* \end{pmatrix} \phi + \text{Tr} A, \\ &\equiv \sum_k \phi^\dagger M \phi + \text{Tr} A, \end{aligned} \quad (23)$$

$$\phi^\dagger \equiv \left(c_{\alpha,k,\uparrow}^\dagger, c_{\alpha,-k,\downarrow} \right), \quad (24)$$

where

$$A^\dagger = A, \quad {}^t B = B. \quad (25)$$

The matrix M is hermite and satisfies the following relations,

$$\sigma_3 \sigma_1 M \sigma_1 \sigma_3 = -M^*, \quad (26)$$

$$M^\dagger = M, \quad (27)$$

where θ is an arbitrary phase factor. We obtain the eigenvalue and the eigenvectors by solving,

$$MV_n = \omega_n V_n \equiv \omega_n \begin{pmatrix} X_n \\ Y_n \end{pmatrix}. \quad (28)$$

By taking account of Eq. (26), the complex conjugate of Eq. (28) satisfies the following equation,

$$M\sigma_1\sigma_3V_n^* = -\omega_n\sigma_1\sigma_3V_n^*. \quad (29)$$

Therefore, $W_n \equiv \sigma_1\sigma_3V_n^*$ is also the eigenvector of M . If V_n belongs to a positive eigenvalue, $\omega_n > 0$, another eigenvector W_n belongs to a negative eigenvalue, $-\omega_n$. By use of b_n^\dagger and b_n defined below,

$$\begin{pmatrix} b_n \\ {}^tb_n^\dagger \end{pmatrix} = \sum \begin{pmatrix} X_{n,\alpha}^* & Y_{n,\alpha}^* \\ -Y_{n,\alpha} & X_{n,\alpha} \end{pmatrix} \begin{pmatrix} c_{\alpha,\uparrow} \\ {}^tc_{\alpha,\downarrow}^\dagger \end{pmatrix}, \quad (30)$$

the Hamiltonian Eq. (23) is diagonalized as,

$$H = 2 \sum_{n>0} \omega_n b_n^\dagger b_n - \sum_{n>0} \omega_n + \text{Tr}A. \quad (31)$$

By using Eq. (30), the electron operator is

$$c_{\alpha,\uparrow} = \sum_n (X_{\alpha,n} b_n - Y_{\alpha,n}^* {}^tb_n^\dagger). \quad (32)$$

The order parameters and the spectral weight are calculated as,

$$\langle 0 | c_{\alpha,\sigma}^\dagger c_{\beta,\sigma} | 0 \rangle = \sum_n Y_{\beta,n}^* Y_{n,\alpha}, \quad (33)$$

$$\langle 0 | c_{\alpha,\sigma}^\dagger c_{\beta,-\sigma}^\dagger | 0 \rangle = \sum_n -X_{\beta,n}^* Y_{n,\alpha}, \quad (34)$$

$$|\langle m | c_{\alpha,\sigma} | 0 \rangle|^2 = \sum_n |Y_{\alpha,n}|^2. \quad (35)$$

[1] H. Ihara, R. Sugise, M. Hirabayashi, N. Terada, M. Jo, K. Hayashi, A. Negishi, M. Tokumoto, Y. Kumira, and T. Shimomura, *Nature* **334**, 510 (1988).
[2] S. S. P. Parkin, V. Y. Lee, A. I. Nazzari, R. Savoy, and R. Beyers, *Phys. Rev. Lett.* **61**, 750 (1988).
[3] J. Kondo, *J. Phys. Soc. Jpn.* **58**, 2884 (1989).
[4] Y. Ohta, T. Tohyama, and S. Maekawa, *Phys. Rev. B* **43**, 2968 (1991).
[5] Y. Ohta and S. Maekawa, *Phys. Rev. B* **41**, 6524 (1990).
[6] M. Di Stasio, K. A. Müller, and L. Pietronero, *Phys. Rev. Lett.* **64**, 2827 (1990).
[7] E. M. Haines and J. L. Tallon, *Phys. Rev. B* **45**, 3172 (1992).
[8] A. Trokiner, L. Le Noc, J. Schneck, A. M. Pougnet, R. Mellet, J. Primot, H. Savary, Y. M. Gao, and S. Aubry, *Phys. Rev. B* **44**, 2426 (1991).
[9] B. W. Statt and L. M. Song, *Phys. Rev. B* **48**, 3536 (1993).

[10] K. Magishi, Y. Kitaoka, G. Aheng, K. Asayama, K. Tokiwa, A. Iyo, and H. Ihara, *J. Phys. Soc. Jpn.* **64**, 4561 (1995).
[11] M.-H. Julien, P. Carretta, M. Horvatić, C. Berthier, Y. Berthier, P. Ségranan, A. Carrington, and D. Colson, *Phys. Rev. Lett.* **76**, 4238 (1996).
[12] H. Kotegawa, Y. Tokunaga, K. Ishida, G. -q. Zheng, Y. Kitaoka, H. Kito, A. Iyo, K. Tokiwa, T. Watanabe, and H. Ihara, *Phys. Rev. B* **64**, 064515 (2001).
[13] G. -q. Zheng, Y. Kitaoka, K. Asayama, K. Hamada, H. Yamauchi, and S. Tanaka, *J. Phys. Soc. Jpn.* **64**, 3184 (1995).
[14] S. Chakravarty, A. Sudbo, P. W. Anderson, S. Strong, *Science* **261**, 337 (1993).
[15] O. K. Andersen, A. I. Liechtenstein, O. Jepsen, and F. Paulsen, *J. Phys. Chem. Solids* **56**, 1573 (1995).
[16] A. I. Liechtenstein, O. Gunnarsson, O. K. Andersen, and R. M. Martin, *Phys. Rev. B* **54**, 12505 (1996).
[17] D. L. Feng, N. P. Armitage, D. H. Lu, A. Damascelli, J. P. Hu, P. Bogdanov, A. Lanzara, F. Ronning, K. M. Shen, H. Eisaki, C. Kim, Z. -X. Shen, J. -i. Shimoyama, and K. Kishio *Phys. Rev. Lett.* **86**, 5550 (2001).
[18] Y. -D. Chuang, A. D. Gromko, A. Fedorov, D. S. Dessau, Y. Aiura, K. Oka, Y. Ando, H. Eisaki, and S. I. Uchida, *Phys. Rev. Lett.* **87**, 117002 (2001).
[19] A. A. Kordyuk, S. V. Borisenko, M. S. Golden, S. Legner, K. A. Nenkov, M. Knupfer, J. Fink, H. Berger, and L. Forro, *cond-mat/0104294*.
[20] D. L. Feng, A. Damascelli, K. M. Shen, N. Motoyama, D. H. Lu, H. Eisaki, K. Shimizu, J. -i. Shimoyama, K. Kishio, N. Kaneko, M. Greven, G. D. Gu, X. J. Zhou, C. Kim, F. Ronning, N. P. Armitage, and, Z. -X. Shen, *cond-mat/0108386*.
[21] T. Sato, H. Matsui, S. Nishina, T. Takahashi, T. Fujii, T. Watanabe, and A. Matsuda, *cond-mat/0108415*.
[22] Y. -D. Chuang, A. D. Gromko, A. V. Fedorov, Y. Aiura, K. Oka, Yoichi Ando, D. S. Dessau, *cond-mat/0107002*.
[23] D. L. Feng, C. Kim, H. Eisaki, D. H. Lu, K. M. Shen, F. Ronning, N. P. Armitage, A. Damascelli, N. Kaneko, M. Greven, J. -i. Shimoyama, K. Kishio, R. Yoshizaki, G. D. Gu, and Z. -X. Shen, *cond-mat/0107073*.
[24] C. Dahnken and R. Eder, *cond-mat/0109036*.
[25] M. Lindroos, S. Sahrakorpi, and A. Bansil, *cond-mat/0109039*.
[26] Y. Tokunaga, K. Ishida, Y. Kitaoka, K. Asayama, K. Tokiwa, A. Iyo, and H. Ihara, *Phys. Rev. B* **61**, 9707 (2000).
[27] H. Suhl, B. T. Matthias, and L. R. Walker, *Phys. Rev. Lett.* **3**, 552 (1959).
[28] C. Kim, P. J. White, Z. -X. Shen, T. Tohyama, Y. Shibata, S. Maekawa, B. O. Wells, Y. J. Kim, R. J. Birgeneau, and M. A. Kastner, *Phys. Rev. Lett.* **80**, 4245 (1998).
[29] T. Tohyama and S. Maekawa, *Supercond. Sci. Technol.* **13**, R17 (2000).
[30] Z. -X. Shen and J. R. Schrieffer, *Phys. Rev. Lett.* **78**, 1771 (1997).
[31] J. C. Campuzano, H. Ding, M. R. Norman, H. M. Fretwell, M. Randeria, A. Kaminsk, *Phys. Rev. Lett.* **83**, 3709 (1999).
[32] P. V. Bogdanov, A. Lanzara, X. J. Zhou, S. A. Kellar, D.

- L. Feng, E. D. Lu, H. Eisaki, J. -I. Shimoyama, K. Kishi, Z. Hussain, and Z.-X. Shen, cond-mat/0005394.
- [33] S. Barnes and S. Maekawa, cond-mat/0111205.
 - [34] Z.-X. Shen and D. S. Dessau, Phys. Rep. **253**, 1 (1995).
 - [35] T. Tanamoto, H. Kohno, and H. Fukuyama, J. Phys. Soc. Jpn. **63**, 2739 (1994).
 - [36] D. L. Feng and Z.-X. Shen, private communication.
 - [37] F. C. Zhang, C. Gros, T. M. Rice, and H. Shiba, Supercond. Sci. Technol. **1**, 36 (1996).
 - [38] M. Ogata and A. Himeta, cond-mat/0003465.
 - [39] R. Eder, Y. Ohta, and S. Maekawa, Phys. Rev. B **51**, 3265 (1995).
 - [40] J.-P. Blaizot and G. Ripka, *Quantum Theory of Finite Systems* (MIT Press, Cambridge, MA, 1986).